International Journal of Pharmaceutics 409 (2011) 314–320

Contents lists available at ScienceDirect

International Journal of Pharmaceutics

journal homepage: www.elsevier.com/locate/ijpharm

Pharmaceutical Nanotechnology

Porphyran capped gold nanoparticles as a novel carrier for delivery of anticancer drug: *In vitro* cytotoxicity study

Vinod Venkatpurwar[a], Anjali Shiras[b], Varsha Pokharkar[a,*]

[a] Department of Pharmaceutics, Bharati Vidyapeeth University, Poona College of Pharmacy, Erandwane, Pune 411038, Maharashtra, India
[b] National Center for Cell Sciences, Pune 411007, Maharashtra, India

ARTICLE INFO

Article history:
Received 24 January 2011
Received in revised form 16 February 2011
Accepted 23 February 2011
Available online 2 March 2011

Keywords:
Porphyran
Gold nanoparticles
Cytotoxicity
Doxorubicin hydrochloride
Drug delivery

ABSTRACT

In the present study, we have explored porphyran as a reducing agent for one pot size controlled green synthesis of gold nanoparticles (AuNps) and further investigated its application as a carrier for the delivery of an anticancer drug. The prepared AuNps showed surface plasmon resonance centered at 520 nm with average particle size of 13 ± 5 nm. FTIR spectra suggested that the sulfate moiety is mainly responsible for reduction of chloroauric acid. The capping of the AuNps with porphyran was evident from the negative zeta potential value responsible for the electrostatic stability. Thus, porphyran acts as reducing as well as capping agent. These AuNps are highly stable in a wide range of pH and electrolyte concentration. Porphyran capped AuNps exhibited enhanced cytotoxicity on human glioma cell line (LN-229) as compared to native porphyran. Consequently, these AuNps have been utilized as a carrier for delivery of the anticancer drug doxorubicin hydrochloride (DOX). Spectroscopic examination revealed that DOX conjugated onto AuNps via hydrogen bonding. The release of DOX from DOX loaded AuNps was found to be sixfold higher in acetate buffer (pH 4.5) as compared to physiological buffer (pH 7.4). Further, the DOX loaded AuNps demonstrated higher cytotoxicity on LN-229 cell line as compared with an equal dose of native DOX solution. This established the potential of these AuNps as a carrier for anticancer drug delivery.

1. Introduction

Novel colloidal carriers such as liposomes, polymeric nanoparticles and solid lipid nanoparticles are widely used for delivery of various biomolecules and pharmaceutical actives because they offer lot of advantages like improved efficacy, targeted delivery and reduced toxicity as compared to conventional drug delivery system (Brigger et al., 2002; RaviKumar, 2000; Han et al., 2007). Metal nanoparticles are new generation materials being widely investigated for biomedical and therapeutic applications. Gold nanoparticles (AuNps) owing to their unique properties such as comparable size with biomolecules, binding ability to various molecules and optical properties in the visible and NIR regions make them potential candidates for chemical as well as biological applications and these can be synthesized easily (Shankar et al., 2005). Recent burst of research includes diagnostic and therapeutic applications of AuNps (Selvakannan et al., 2004; Mirkin et al., 1996; Tsai et al., 2004). For such purpose several researchers improved the properties of biomolecules and drugs such as amino acids (Hainfeld et al., 2004), protein (Gole et al., 2001), DNA (Alivisatos et al., 1996), insulin (Joshi et al., 2006), ciprofloxacin (Tom et al., 2004) and plasmid (Thomas and Klibanov, 2003) after conjugation with AuNps synthesized by conventional route. These conventional methods utilized sodium borohydride or tri-sodium citrate like harsh reducing agents. The drawbacks of these methods are that the nanoparticles are unstable and form aggregates at the slightest change in their pH and electrolyte environments (Rouhana et al., 2007). To overcome such tedious techniques and utilization of harsh reducing agents, the interest in this field has shifted towards 'green' chemistry and bioprocess approach. This approaches focus on exploration of cost effective eco friendly and biocompatible reducing agents for synthesis of AuNps. Early report cite the use of several plant extracts such as coriander (Narayanan and Sakthivel, 2008), banana peel (Bankar et al., 2010), *Barbated skullcup* herb (Wang et al., 2009) and *Syzygium cumini* leaf (Kumar et al., 2010) for synthesis of AuNps. Recently, *Bacillus subtilis* and *Rhodopseudomonas capsulate* like microorganism (Reddy et al., 2010; He et al., 2007) were utilized for the biosynthesis of AuNps. However, these natural sources containing several components generate AuNps at much slower rate over a period of 24–48 h. To this end, interest in this field has increased by utilizing non-toxic and biocompatible naturally occurring polysaccharides such as chitosan (Bhumkar et al., 2007) and gellan gum (Dhar et al., 2008) for rapid synthesis of AuNps and subsequent use for drug delivery applications.

* Corresponding author. Tel.: +91 20 25437237; fax: +91 20 25439383.
E-mail address: vbpokharkar@yahoo.co.in (V. Pokharkar).

0378-5173/$ – see front matter © 2011 Elsevier B.V. All rights reserved.
doi:10.1016/j.ijpharm.2011.02.054

Porphyran, a sulfated polysaccharide is obtained from marine red algae (*Porphyra vietnamensis*) (Dinabandhu et al., 2006). Porphyran comprising the hot-water soluble portion of cell wall is the main component of the marine red algae. Porphyran comprises of anionic disaccharide units consisting of 3-linked-D-galactosyl residues alternating with 4-linked 3,6-anhydro-L-galactose and the 6-sulfate residues (Gretz et al., 1983; Morrice et al., 1983). Porphyran is a dietary fiber that contains about 40–50% of seaweed components. Pharmacological functions of isolated porphyran from several porphyra species were demonstrated in different structural and functional studies. It was interesting to note the reports on the antioxidant and anticancer activity of porphyran (Zhang et al., 2003; Kwon and Nam, 2006). Pursuing our interest we have explored the use of porphyran for one pot size controlled green synthesis of AuNps. We hypothesized that the anticancer activity of porphyran may improve after capping on AuNps. Further, capping of carbohydrate rich porphyran on AuNps may improve its functionality for conjugation with biological molecules. To demonstrate applicability of these nanoparticles for drug delivery we have investigated the loading of anticancer drug doxorubicin hydrochloride (DOX) on porphyran reduced AuNps. DOX is a potent anthracycline antibiotic used for various cancer therapies such as malignancies, carcinoma and sarcomas, Lack of tumor targeting capacity of DOX results in narrow biodistribution and undesirable side effects which remain as major problems to be solved (Steiniger et al., 2004). This led the company ALZA to develop a product DOXIL® that improved the performance by encapsulating the DOX in a liposome, thereby enhancing the anticancer action of DOX (Ning et al., 2007; Ogawara et al., 2008).

Here, we report the green synthesis of AuNps using porphyran and subsequently loading of DOX. The porphyran reduced AuNps and DOX loaded AuNps were evaluated through suitable techniques to study morphology, surface charge and drug loading efficiency. Further, we analyzed the functional group responsible for reduction of chloroauric acid through Fourier transform infrared spectroscopy method. Effect of pH condition and presence of electrolyte on these AuNps was carried out. Six month stability study of these nanoparticles was performed at ambient temperature. *In vitro* cytotoxicity study on human glioma cell line (LN-229) was carried out for porphyran capped AuNps and DOX loaded AuNps by MTT assay. *In vitro* release studies of DOX loaded AuNps was carried out in different pH to demonstrate the effect of pH on the release of DOX.

2. Experimental

2.1. Materials and reagents

Doxorubicin hydrochloride was gifted from RPG Life Sciences Ltd. (Mumbai, India). Hydrochloroauric acid ($HAuCl_4$) was purchased from Sisco India Ltd. (Mumbai, India). The human glioma cell line (LN-229) was procured from American type culture collection (ATCC, USA). The yellow tetrazolium MTT (3-(4,5-dimethylthiazolyl-2)-2,5-diphenyltetrazolium bromide) was purchased from Sigma–Aldrich (USA). Analytical grade reagents are taken from Merck India Ltd. (Mumbai, India). All the samples were prepared in deionized water.

2.2. Synthesis of gold nanoparticles

The porphyran were isolated form marine red algae (*P. vietnamensis* species) using reported method (Nishide et al., 1988; Ishihara et al., 2005) and this species of marine red algae was collected in rainy season on the west coast of India, especially in the provinces of Maharashtra, Goa and Karnataka. The isolated porphyran was characterized using established methods (S1 in supporting information). The 0.01% (w/v) of isolated porphyran was added to 100 mL aqueous solution of $HAuCl_4$ (1×10^{-4} M) and pH of solution was adjusted at 11 to yield dark ruby red AuNps on heating for 15 min at 70 °C on water bath. The AuNps dispersion was dialyzed using dialysis tubing (12 kDa cut off) for 24 h to remove the ionic impurities. After dialysis, the pH of the AuNps dispersion was measured to be 7.

2.3. UV/Visible spectroscopy measurement

The UV/Visible spectra of native porphyran solution (0.1% (w/v)) and porphyran reduced AuNps was monitored by UV/Visible spectroscopy (Jasco Dual Beam UV/Visible Spectrophotometer, Japan).

2.4. Loading of doxorubicin hydrochloride onto gold nanoparticles

A calculated amount of DOX was added to AuNps dispersion (pH 7), obtained as described above, resulting in a final DOX concentration of 10^{-4} M in solution. The mixture of DOX and AuNps dispersion was incubated for 24 h at room temperature and then centrifuged at 10,000 rpm for 15 min. The obtained pellet after centrifugation was separated from the supernatant solution and redispersed in deionized water prior to further characterization.

2.5. Determination of percent drug loading on to gold nanoparticles

Drug loading was calculated by two ways, first based on indirect method by estimating the DOX content of the supernatant and second based on direct estimation of the DOX content present in the pellet obtained after centrifugation. The drug concentration in supernatant and redispersed pellet were determined by measurements of its UV absorbance at 480 nm using UV/Visible spectroscopy and the percentage loading of DOX on to AuNps was estimated by the following formula

$$\% \text{ Loding} = \frac{\text{Total amount of DOX added} - \text{amount of DOX in supernatent or redispersed pellet}}{\text{Total amount of DOX added}} \times 100$$

2.6. Characterization of gold nanoparticles and DOX loaded gold nanoparticles

Fourier transform infrared (FTIR) spectra of native porphyran, porphyran reduced AuNps, native DOX and DOX loaded AuNps was recorded in KBr pellets using FTIR spectrophotometer (Jasco, Japan). The scan was performed in the range 400–4000 cm^{-1}. The morphology and size distribution of the porphyran reduced AuNps and DOX loaded AuNps dispersion was carried out by high resolution transmission electron microscopy (HRTEM) measurement casting of nanoparticle dispersion on carbon-coated copper grids and allowed to dry at room temperature. Measurements were done on TECHNAI G^2 F30 S-TWIN instrument operated at an accelerated voltage of 200 kV with a lattice resolution of 0.14 nm and point image resolution of 0.20 nm. The particle size analysis was carried out using Gattan software (Pleasanton, CA, USA). The hydrodynamic diameter of AuNps was determined using Zetasizer 300 HAS (Malvern, UK). Analysis ($n = 3$) was carried out at room temperature by keeping angle of detection at 90°. Particle size of the sample was measured as such without dilution. X-ray diffraction (XRD) measurement of porphyran reduced AuNps was carried out by preparing films of nanoparticle dispersion on glass substrates by simple solvent evaporation method at room temperature. The

diffraction measurements were carried out on X'pert Pro X-ray diffractometer (Netherland) instrument operating at 40 kV and a current of 30 mA at a scan rate of 0.388/min. The zeta potential of AuNps before and after loading of DOX was determined by using the Zetasizer 300 HAS (Malvern, UK) as such without dilution.

2.7. Stability study of gold nanoparticles

The stability study of porphyran reduced AuNps was carried out at ambient temperature. The change in surface plasmon resonance (SPR) of the nanoparticle dispersion was recorded up to six month using UV/Visible spectroscopy.

2.8. pH and electrolytic stability study of gold nanoparticles

In the pH stability study, the pH of AuNps dispersion was adjusted using 0.1 N hydrochloric acid (pH 2, 3, 4, 5 and 6) and 0.1 M sodium hydroxide (pH 7, 8, 9, 10, 11 and 12) using calibrated pH meter (Delux pH Meter 101, India). Change in SPR of AuNps dispersion was recorded after 24 h using an UV/Visible spectrophotometer. Also, the effect of electrolyte was studied by adding varying molar concentration of sodium chloride (10^1 to 10^{-6} M) to AuNps dispersion. The change in SPR was recorded after 24 h using UV/Visible spectrophotometer.

2.9. In vitro cytotoxicity study

Human glioma cell line (LN-229) was cultured in Dulbecco's modified eagle's medium (DMEM) supplemented with 1.5 g/mL sodium bicarbonate, 4 mm glutamine and 5–10% fetal bovine serum (Gibco, USA). The cultures were maintained in a humidified atmosphere of 5% CO_2 at 37 °C in an incubator. For cytotoxicity testing, the cells were utilized when they reached 70–80% confluence. The cells were diluted as needed and seeded as 3×10^3 for LN-229 in 200 μL of media per well, sequentially plated in flat bottom 96 well plates (Becton Dickinson Labwane, USA). This number of cells was selected to avoid potential over confluence of the cells at the end of the four day experiment while still providing enough cells for adequate formazan production. After plating, the 96 well plates were then incubated for 24 h to allow adherence of the cells prior to the administration of various samples for testing. After complete adherence of cells the culture medium was replaced with 200 μL of solution containing mixture of fresh medium and porphyran solution prepared in deionized water (0.01% (w/v)), porphyran capped AuNps dispersion, native DOX solution prepared in deionized water and DOX loaded AuNps in separate wells. Control wells containing cells received only 200 μL of medium. After addition of all the test samples, the plates were incubated up to 72 h for native porphyran and porphyran capped AuNps and 48 h for unloaded AuNps, native DOX and DOX loaded AuNps in CO_2 incubator. The cells could be maintained in wells for this period without the need for refeeding. All experiments were performed in triplicate. MTT assay was based on the measurement of the mitochondrial activity of viable cells by the reduction of the tetrazolium salt MTT (3-(4,5-dimethyathiazol-2-yl)-2,5-diphenyl tetrazolium bromide) to form a blue water-insoluble product, formazan. MTT (5 mg/mL, 20 μL) was added to respective set of cells and the plates were incubated for an additional 4 h. After 4 h of incubation, the medium was removed and DMSO (200 μL, Sigma–Aldrich, USA) was added to dissolve the formazan crystals resulting from the reduction of the tetrazolium salt only by metabolically active cells (Mosmann, 1983; Kleihues and Ohgaki, 2000; Kleihues et al., 2002). The absorbance of dissolved formazan was measured at 570 nm using a Bio-Rad microplate reader (Model 680, Heraeus, USA). Since the absorbance directly correlated with the number of viable cells, the percent viability was calculated from the absorbance.

2.10. Statistical analysis

Data was expressed as mean ± S.D. and statistical analysis was carried out using two way ANOVA followed by Bonferroni post test. A level of significance of $p < 0.0001$ was regarded as statistically significant.

2.11. In vitro drug release study of doxorubicin loaded gold nanoparticles

The dialysis tube containing DOX loaded AuNps was transferred to a beaker containing 100 mL of phosphate buffer (pH 7.4) by maintain temperature at 37 °C with continuous stirring at 100 rpm. Sink condition was maintained by periodically removing 2 mL sample and replacing equal volume of buffer. The amount of DOX release was analyzed with a spectrophotometer at 485 nm. A similar release study was carried out in acetate buffer (pH 4.5). The experiments were performed in triplicate for each of the samples.

3. Results and discussion

In this work, we have utilized isolated porphyran as a reducing as well as stabilizing agent for the one pot size controlled green synthesis of AuNps. Further, we have investigated that these synthesized AuNps would enable attachment of biomolecules for drug delivery applications (Scheme 1).

3.1. Synthesis and evaluation of gold nanoparticles

Preliminary study revealed that the reduction of gold ions in presence of porphyran did not occur in deionised water and up to pH 7 on heating for 10 min, but as pH increased to 11 reduction occurred as indicated by the color change. At pH 11 the color of solution changed from colorless to dark ruby red on heating for 10 min (inset Fig. 1a). Fig. 1a shows the UV/Visible spectra recorded from the dispersion obtained by the reduction of $HAuCl_4$ using 0.01% (w/v) of porphyran at pH 11, the band corresponding to the SPR occurred at 520 nm. SPR of AuNps appears in the visible region and can be used to monitor shape, size and aggregation of the nanoparticles (Bhumkar et al., 2007). It was observed that $HAuCl_4$ reduction occurs rapidly and the intensity remained unchanged, without any shift in the peak wavelength even after 24 h of reduction time. The FTIR spectra of porphyran (Fig. 1b(I)) depicted typical bands at 1645, 1417, 1230, 1158, 1019, 933 and 819 cm^{-1}. The signal at 1230 cm^{-1} was assigned to the asymmetric stretching vibration of sulfate group and the band at 819 cm^{-1} was indicative of a sulfate group attached to a primary hydroxyl group. Another weak band at 933 cm^{-1} was due to the 3,6-anhydro-D-galactose unit in the porphyran. From these results and similar finding reported earlier we confirmed that the isolated porphyran contained 3,6-anhydro-D-galactose unit and sulfate group (Brasch et al., 1981; Zhang et al., 2009). Fig. 1b(II) depicted the FTIR spectra of porphyran reduced AuNps, where signal of asymmetric stretching vibration of sulfate group shifted from 1230 cm^{-1} to 1283 cm^{-1} while the signal at 819 cm^{-1} (sulfate group attached to a primary hydroxyl group) disappeared after synthesis of AuNps indicating the involvement of the sulfur group of porphyran in the reduction process. HRTEM images (Fig. 2a) revealed that the porphyran reduced AuNps appeared to be spherical in shape with narrow size distribution and inset Fig. 2a showed average particle size about 13 ± 5 nm. The selected area of electron diffraction pattern of obtained AuNps showing the rings designated 1, 2, 3 and 4 arise due to the reflections from (1 1 1), (2 0 0), (2 2 0) and (3 1 1) (Fig. 2b). This was further confirmed by the powder X-ray diffractogram recorded from the sample (inset Fig. 2b), which indexed as the band for face centered cubic (fcc) structures of gold. The XRD pattern thus illustrated

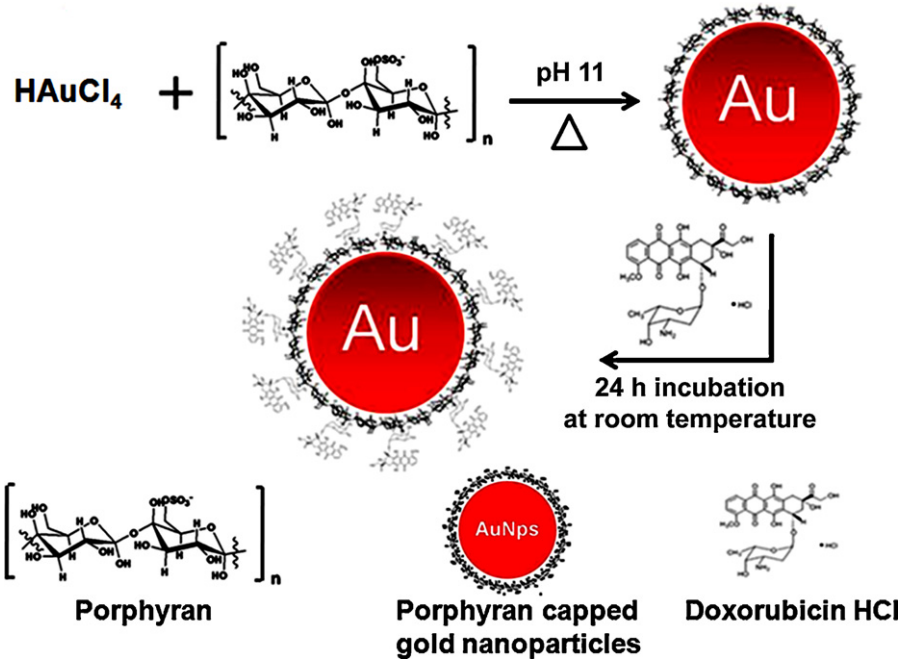

Scheme 1. Schematic representation showing porphyran reduced gold nanoparticles (AuNps) and subsequent loading of cationic doxorubicin HCl on porphyran capped gold nanoparticles.

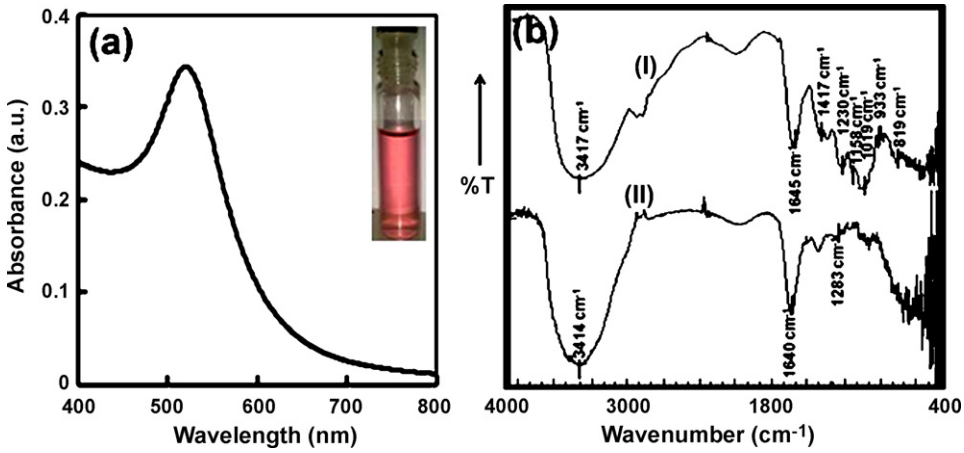

Fig. 1. (a) UV/Visible spectra of 0.01% (w/v) porphyran reduced gold nanoparticles (AuNps) and inset photograph showed ruby red color of AuNps dispersion, (b) FTIR spectra of (I) isolated porphyran and (II) porphyran reduced AuNps. (For interpretation of the references to color in this figure legend, the reader is referred to the web version of this article.)

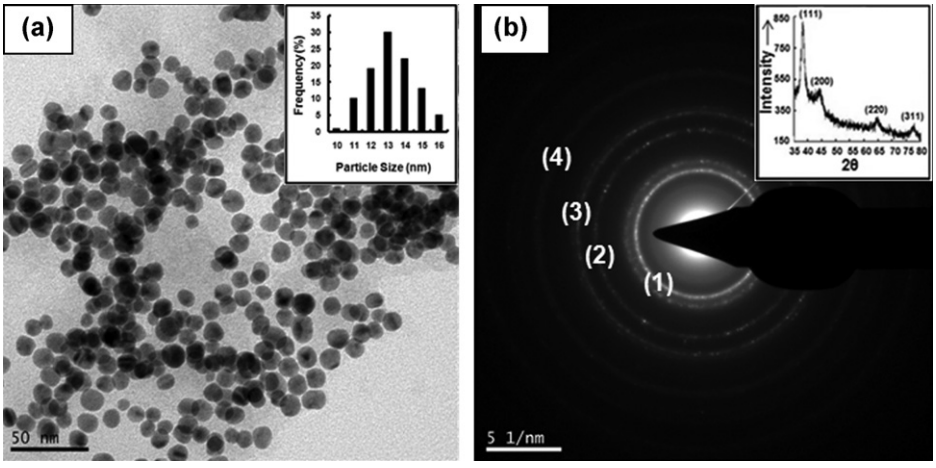

Fig. 2. (a) HRTEM images of porphyran reduced AuNps and inset image showed particle size distribution graph, and (b) electron diffraction pattern of porphyran reduced AuNps and inset image showed XRD pattern of porphyran reduced AuNps.

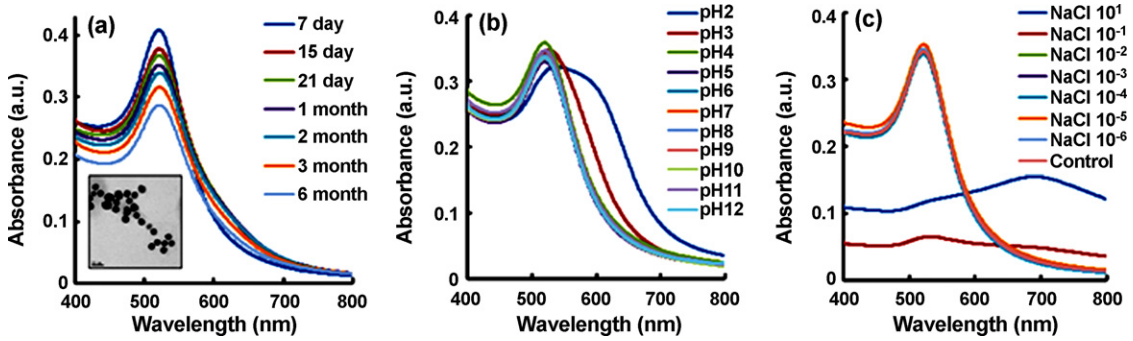

Fig. 3. UV/Visible spectra of porphyran reduced AuNps (a) of six month stability study (inset showed HRTEM image of six months stability sample of AuNps) (b) at varied pH conditions and (c) electrolytic concentration.

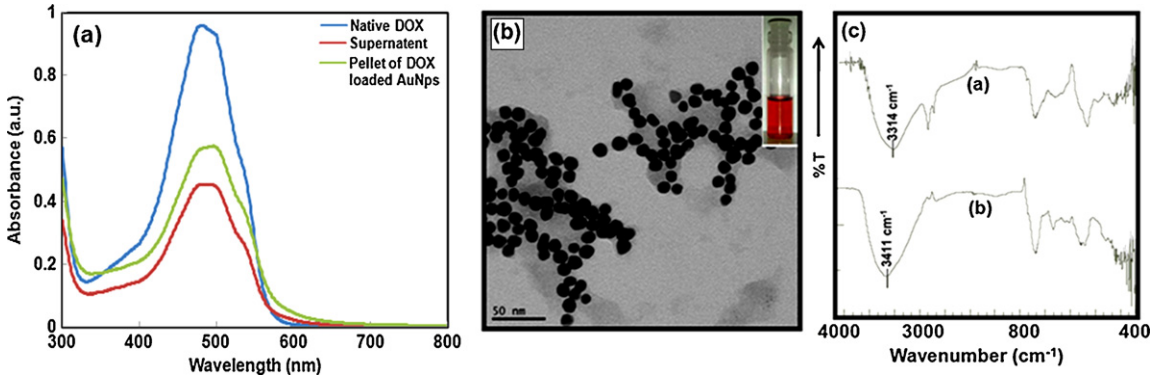

Fig. 4. (a) UV/Visible spectra of native DOX solution, redispersed pellet of DOX loaded AuNps and supernatant of DOX loaded AuNps, (b) HRTEM image of doxorubicin (DOX) loaded AuNps and inset photograph represented color of redispersed DOX loaded AuNps and (c) FTIR spectra of (a) native DOX and (b) DOX loaded AuNps.

the broadening of Bragg's peaks which is indication of crystalline nanoparticles (Narayanan and Sakthivel, 2008). The hydrodynamic particle size of the 0.01% (w/v) porphyran reduced AuNps was found to be 101 ± 4 nm with polydispersity index of 0.119. Low polydispersity index indicates the uniformity of particle size distribution. Zeta potential of porphyran reduced AuNps was found to be −31.05 mV. The negative charge indicated that the AuNps were properly capped with anionic porphyran. In general, particle aggregation is less likely to occur for charged particles with optimum zeta potential (∼±30 mV) due to electrostatic repulsions (Bhumkar et al., 2007). Thus, porphyran acts as reducing as well as capping agent.

3.2. Stability study at wide range of pH condition and electrolytic concentration

For varied therapeutic and biomedical applications, we performed the stability study of porphyran reduced AuNps by monitoring the SPR over reasonable period of time and under different pH and electrolytic conditions. It should be noted that a red shift in UV/Visible spectra is mainly associated with either an increase in the mean size of the particles or aggregation of nanoparticles or a combination of both (Sato et al., 2003). Noticeable variation in UV/Visible spectra and particle size of porphyran capped AuNps was not observed over six month stability period revealed that these AuNps are highly stable over reasonable period of time (Fig. 3a). Further, these nanoparticles did not show any SPR shift and change in peak intensity over the pH range of 3–12 and up to 1×10^{-2} M concentration of electrolyte (NaCl) after 24 h incubation at ambient temperature, respectively (Fig. 3b and c). Such insignificant change in its position under pH change and electrolytic conditions indicated greater stability of porphyran reduced AuNps as compared to borohydrate or citrate reduced AuNps aggregate (Rouhana et al., 2007). All these results laid out the utility of these nanoparticles for drug delivery application.

3.3. Evaluation of doxorubicin loaded gold nanoparticles

After the successful synthesis of stable AuNps, we have envisaged this system for drug delivery application through subsequent loading of a bioactive molecule. Using a delivery system with non-covalently loaded drug is considered a more rationale approach that avoids any potential issues associated with a prodrug strategy. We have selected anticancer drug DOX (doxorubicin hydrochloride) ($pK_a = 8.2$) for loading on synthesized AuNps. Percent loading of DOX on to AuNps was determined based on DOX content in the supernatant and obtained pellet and it was found to be $38 \pm 3\%$ and $60 \pm 4.5\%$ of DOX, respectively (Fig. 4a). Fig. 4b represented HRTEM image of DOX loaded AuNps revealed insignificant change in particle size (14 ± 3 nm) and inset image represented uniformly redispersed DOX loaded AuNps dispersion. The hydrodynamic particle size of the DOX loaded AuNps was found to be 105 ± 2 nm with polydispersity index of 0.329. The decrease in the zeta potential (from −31.05 mV to −19 mV) of DOX loaded AuNps was ascribed to the presence of positively charged DOX on the surface of AuNps. It was thought that along with the electrostatic interaction other attractive forces including hydrogen bond could be playing a major role facilitating the drug loading process. The hydrogen bonding between protonated amine groups of the DOX molecule with porphyran on the surface of AuNps is evidenced by FTIR, where NH stretching band at 3314 cm^{-1} of native DOX shifted to 3413 cm^{-1} in case of DOX loaded AuNps (Fig. 4c).

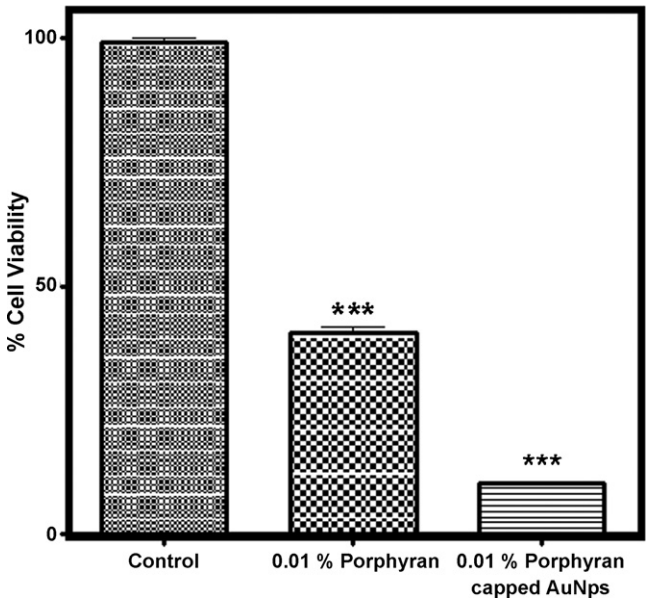

Fig. 5. Percent cell viability of human glioma cell line (LN-229) after exposure to 0.01% porphyran and 0.01% porphyran capped AuNps at the end of 72 h.

3.4. In vitro cytotoxicity study

In order to demonstrate the cytotoxic effect of the porphyran capped AuNps, we have performed cytotoxicity study of (0.01% (w/v)) native porphyran and (0.01% (w/v)) porphyran capped AuNps on LN-229 cell line using *in vitro* MTT assay method. At the end of 72 h, we observed that both native porphyran and porphyran capped AuNps decreased the cell viability. It was interesting to note a fourfold increase in cytotoxicity of porphyran capped AuNps as compared to native porphyran ($p < 0.0001$) (Fig. 5). This clearly demonstrated the role of AuNps for the enhancement of cytotoxic effect of porphyran on human glioma cell line. Previous report justified that porphyran exhibited cytotoxicity on human gastric carcinoma cell line via induction of apoptosis related signaling through activation of proapoptotic molecules (Bax and caspase-3), suppression of anti-apoptotic molecule (Bcl-2), inhibition of IGF-I receptor and decrease in the level of Akt activation (Kwon and Nam, 2006). In our case, improvement in cytotoxicity of porphyran capped AuNps can be attributed to the greater uptake potential of the AuNps by endocytosis mechanism as compared to native porphyran (Dhar et al., 2008; Chen et al., 2007).

Further, to establish the capabilities of the synthesized AuNps as an efficient drug carrier, we determined the cytotoxicity of native DOX solution and DOX loaded AuNps on LN-229 cell line using *in vitro* MTT assay method. Fig. 6a illustrates cytotoxic effect of unloaded AuNps and DOX in the form of either DOX loaded AuNps or native DOX on the LN-229 cells after 48 h exposure. The concentration of DOX loaded AuNps was equivalent to the concentration of native DOX solution. The unloaded AuNps at a dose equivalent to the higher dose of DOX loaded AuNps (15 μg/mL and above) showed 80% cell viability at the end of 48 h. This could be attributed to the cytotoxic effect of porphyran capped on the surface of AuNps on the human cancer cell line. However at lower doses of unloaded AuNps insignificant cytotoxicity was observed. Both, native DOX and DOX loaded AuNps decreases cell viability with increasing concentration of DOX. However, it was observed that the cytotoxicity of DOX loaded AuNps was statistically dominating as compared to native DOX ($p < 0.001$). At the end of 48 h, the decrease in cell viability with native DOX and DOX loaded AuNps in the concentration range studied (1.0–20 μg/mL) was found to be between 60–35% and 45–15%, respectively. Previously, Serpe et al. reported higher cytotoxicity of DOX when incorporated in solid lipid nanoparticles as compared to native DOX solution and they have justified that such increase in cytotoxicity of DOX may be due to the fast internalization of DOX loaded solid lipid nanoparticles followed by the release of DOX inside the cells (Serpe et al., 2004). In our study, it was observed that a significant increase in the cytotoxicity of DOX on LN-229 when loaded on AuNps compared to native DOX. The increase in cytotoxicity of DOX loaded AuNps may be due to the enrichment in internalization of DOX loaded AuNps by an endocytosis mechanism as compared to the passive diffusion mechanism of native DOX into cells (Yoo et al., 2000). In an earlier cytotoxicity study of anticancer drug loaded AuNps, Chen et al. have reported the intracellular accumulation of methotrexate conjugated AuNps owing to AuNps mediated endocytosis (Chen et al., 2007).

3.5. In vitro drug release study of doxorubicin loaded gold nanoparticles

The ability of the carrier to release the cargo efficiently at the desired site is an important feature of any delivery system. Fig. 6b depicts the release of DOX from DOX loaded AuNps in acetate buffer (pH 4.5) and phosphate buffer (pH 7.4). At the end of 7 h, 98% and 15% of DOX was released in acetate and phosphate buffer, respectively. This revealed that the release of DOX was higher in acidic pH as compared to basic pH. This pH dependant release may help to improve efficacy of DOX since the uptake of drug loaded nanopar-

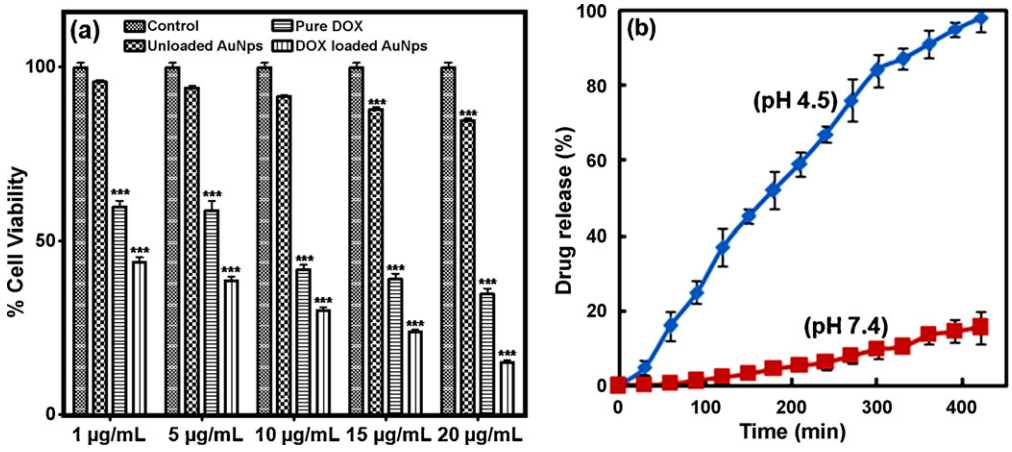

Fig. 6. (a) Percent cell viability of LN-229 cell line after exposure to control media, unloaded AuNps, native DOX solution and DOX loaded AuNps (48 h) and (b) the drug release profile of DOX from DOX loaded AuNps in acetate buffer (pH 4.5) and phosphate buffer (pH 7.4).

ticle through endocytosis process leads to exposure to an acidic environment (Bareford and Swaan, 2007). This may initiate rapid release of DOX from DOX loaded AuNps after internalization. Such efficient release would ultimately result in improved cytotoxic efficacy against tumor cells. Also, negligible release of DOX from DOX loaded AuNps in basic pH will help to reduce toxicity of DOX to the normal tissue since the physiological pH of body is maintained at pH 7.4 (Santosh et al., 2009).

4. Conclusion

In conclusion, we have reported size controlled one pot green synthesis of AuNps by using isolated porphyran. These nanoparticles exhibited stability in a wide range of pH and electrolyte concentration. Further, applicability of these nanoparticles as a carrier for the delivery of the cationic anticancer drug was demonstrated by successful loading of DOX onto synthesized AuNps. Enhanced cytotoxicity of DOX loaded AuNps can be attributed to the greater uptake potential of the AuNps thus establishing the role of the gold nanoparticle as an efficient carrier for the delivery of anticancer drug. These DOX loaded AuNps exhibited a pH dependant release behavior with negligible release of DOX in basic pH which may help to reduce the toxicity of DOX to the normal tissue. Further, *in vivo* toxicity study of porphyran capped AuNps and *in vivo* anti-tumor activity of DOX loaded AuNps are under investigation in our laboratory.

Acknowledgement

Vinod Venkatpurwar would like to thank All India Council for Technical Education (AICTE), Delhi, India for providing National doctoral fellowship (NDF). Authors would like to thank Dr. B.L.V. Prasad for providing the facility for HRTEM analysis.

Appendix A. Supplementary data

Supplementary data associated with this article can be found, in the online version, at doi:10.1016/j.ijpharm.2011.02.054.

References

Alivisatos, A.P., Peng, X., Wilson, T.E., Loweth, C.L., Bruchez Jr., M.P., Schultz, P.G., 1996. Organization of 'nanocrystal molecules' using DNA. Nature 382, 609–611.
Bankar, A., Joshi, B., Kumar, A.R., Zinjarde, S., 2010. Banana peel extract mediated synthesis of gold nanoparticles. Colloids Surf. B 80, 45–50.
Bareford, L.M., Swaan, P.W., 2007. Endocytic mechanisms for targeted drug delivery. Adv. Drug. Deliv. Rev. 59, 748–758.
Bhumkar, D., Joshi, H., Sastry, M., Pokharkar, V., 2007. Chitosan reduced gold nanoparticles as novel carriers for transmucosal delivery of insulin. Pharm. Res. 24, 1415–1426.
Brasch, D.J., Chang, H.M., Chuah, C.T., Melton, L.D., 1981. The galactan sulfate from the edible, red alga *Porphyra columbina*. Carbohydr. Res. 97, 113–125.
Brigger, I., Dubernet, C., Couvreur, P., 2002. Nanoparticles in cancer therapy and diagnosis. Adv. Drug. Deliv. Rev. 54, 631–651.
Chen, Y., Tsai, C., Huang, P., Chang, M., Cheng, P., Chou, C., Chen, D., Wang, C., Shiau, A., Wu, C., 2007. Methotrexate conjugated to gold nanoparticles inhibits tumor growth in a syngeneic lung tumor model. Mol. Pharm. 4, 713–722.
Dhar, S., Reddy, E.M., Shiras, A., Pokharkar, V., Prasad, B.L.V., 2008. Natural gum reduced/stabilized gold nanoparticles for drug delivery formulations. Chem. Eur. J. 14, 10244–10250.
Dinabandhu, S., Baweja, P., Kushwah, N., 2006. Developmental studies in *Porphyra vietnamensis*: a high-temperature resistant species from the Indian coast. J. Appl. Phycol. 18, 279–286.
Gole, A., Dash, C., Ramakrishnan, V., Sainkar, S.R., Mandale, A.B., Rao, M., Sastry, M., 2001. Pepsin–gold colloid conjugates: preparation, characterization, and enzymatic activity. Langmuir 17, 1674–1679.
Gretz, M.R., McCandless, E.L., Aronson, J.M., Sommerfeld, M.R., 1983. The galactan sulphates of the conchocelis phases of *Porphyra leucostricta* and *Bangia atropurpurea* (Rhodophyta). J. Exp. Bot. 34, 705–711.
Hainfeld, J.F., Slatkin, D.N., Smilowitz, H.M., 2004. The use of gold nanoparticles to enhance radiotherapy in mice. Phys. Med. Biol. 49, N309.
Han, G., Ghosh, P., Rotello, V., 2007. Functionalized gold nanoparticles for drug delivery. Nanomedicine 2, 113–123.
He, S., Guo, Z., Zhang, Y., Zhang, S., Wang, J., Gu, N., 2007. Biosynthesis of gold nanoparticles using the bacteria Rhodopseudomonas capsulate. Mater. Lett. 61, 3984–3987.
Ishihara, K., Oyamada, C., Matsushima, R., Muratam, M., Muraoka, T., 2005. Inhibitory effect of porphyran prepared from dried nori on contact hypersensitivity in mice. Biosci. Biotechnol. Biochem. 69, 1824–1830.
Joshi, H.M., Bhumkar, D.R., Joshi, K., Pokharkar, V.B., Sastry, M., 2006. Gold nanoparticles as carriers for efficient transmucosal insulin delivery. Langmuir 2, 300–305.
Kleihues, P., Ohgaki, H., 2000. Phenotype vs genotype in the evolution of astrocytic brain tumors. Toxicol. Pathol. 28, 164–170.
Kleihues, P., Louis, D.N., Scheithauer, B.W., Rorke, L.B., Eifenberger, G., Burger, P.C., Cavenee, W.K., 2002. The WHO classification of tumors of the nervous system. J. Neuropathol. Exp. Neurol. 61, 215–225.
Kumar, V., Yadav, S.C., Yada, S.K., 2010. *Syzygium cumini* leaf and seed extract mediated biosynthesis of silver nanoparticles and their characterization. J. Chem. Technol. Biotechnol. 85, 1301–1309.
Kwon, M.J., Nam, T.J., 2006. Porphyran induces apoptosis related signal pathway in AGS gastric cancer cell lines. Life Sci. 79, 1956–1962.
Mirkin, C.A., Letsinger, R.L., Mucic, R.C., Storhoff, J.J., 1996. A DNA-based method for rationally assembling nanoparticles into macroscopic materials. Nature 382, 607–609.
Morrice, L.M., Mclean, M.W., Long, W.F., Williamson, F.B., 1983. Porphyran primary structure. Eur. J. Biochem. 133, 671–684.
Mosmann, T., 1983. Rapid colorimetric assay for cellular growth and survival: application to proliferation and cytotoxicity assays. J. Immunol. Methods 65, 55–63.
Narayanan, K.B., Sakthivel, N., 2008. Coriander leaf mediated biosynthesis of gold nanoparticles. Mater. Lett. 62, 4588–4590, http://linkinghub.elsevier.com/retrieve/pii/S0167577X08007416.
Ning, Y.M., He, K., Dagher, R., Sridhara, R., Farrell, A., Justice, R., Padzur, R., 2007. Liposomal doxorubicin in combination with bortezomib for relapsed or refractory multiple myeloma. Oncology 21, 1503–1508.
Nishide, E., Ohno, M., Anzia, H., 1988. Extraction of porphyra yezonensis U_{EDA} F. arawaensis$_{IURA}$, N. Uchida. Nippon Suisan Gakkaishi 54, 2189–2194.
Ogawara, E., Un, K., Minato, K., Tanaka, K., Higaki, K., Kimura, T., 2008. Determinants for in vivo anti-tumor effects of PEG liposomal doxorubicin: importance of vascular permeability within tumors. Int. J. Pharm. 359, 234–240.
RaviKumar, M.N.V., 2000. Nano and microparticles as controlled drug delivery devices. J. Pharm. Pharm. Sci. 3, 234–558.
Reddy, A.S., Chen, C.Y., Chen, C.C., Jean, J.S., Chen, H.R., Tseng, M.J., Fan, C.W., Wang, J.C., 2010. Biological synthesis of gold and silver nanoparticles mediated by the bacteria *Bacillus subtilis*. J. Nanosci. Nanotechnol. 10, 6567–6574.
Rouhana, L.L., Jaber, J.A., Schlenoff, J.B., 2007. Aggregation-resistant water-soluble gold nanoparticles. Langmuir 23, 12799–12801.
Santosh, A., Grailer, J.J., Pilla, S., Douglas, A.S., Gong, S., 2009. Doxorubicin conjugated gold nanoparticles as water-soluble and pH-responsive anticancer drug nanocarriers. J. Mater. Chem. 19, 7879–7884.
Sato, K., Hosokawa, K., Maeda, M., 2003. Rapid aggregation of gold nanoparticles induced by non-cross-linking DNA hybridization. J. Am. Chem. Soc. 125, 8102–8103.
Selvakannan, P.R., Mandal, S., Phadtare, S., Gole, A., Pasricha, R., Adyanthaya, S.D., Sastry, M., 2004. Water-dispersible tryptophan-protected gold nanoparticles prepared by the spontaneous reduction of aqueous chloroaurate ions by the amino acid. J. Colloid Interface Sci. 269, 97–102.
Serpe, L., Catalano, M.G., Cavalli, R., Ugazio, E., Bosco, O., Canaparo, R., Muntoni, E., Frairia, R., Gasco, M.R., Eandi, M., Zara, G.P., 2004. Cytotoxicity of anticancer drugs incorporated in solid lipid nanoparticles on HT-29 colorectal cancer cell line. Eur. J. Pharm. Biopharm. 58, 673–680.
Steiniger, S.C.J., Kreuter, J., Khalansky, A.S., Skdan, I.N., Bobruskin, A.I., Smirnova, Z.S., Severin, S.E., Uhl, R., Kock, M., Geiger, K.D., Gelperina, S.E., 2004. Chemotherapy of glioblastoma in rats using doxorubicin-loaded nanoparticles. Int. J. Cancer 109, 759–767.
Shankar, S.S., Rai, A., Ahmad, A., Sastry, M., 2005. Controlling the optical properties of lemongrass extract synthesized gold nanotriangles and potential application in infrared-absorbing optical coatings. Chem. Mater. 17, 566–572.
Thomas, M., Klibanov, A.M., 2003. Conjugation to gold nanoparticles enhances polyethylenimines transfer of plasmid DNA into mammalian cells. Proc. Natl. Acad. Sci. U. S. A. 100, 9138–9143.
Tom, R.T., Suryanarayanan, V., Reddy, P.G., Baskaran, S., Pradeep, T., 2004. Ciprofloxacin-protected gold nanoparticles. Langmuir 20, 1909–1914.
Tsai, C.Y., Shiau, A.L., Cheng, P.C., Shieh, D.B., Chen, D.H., Chou, C.H., Yeh, C.S., Wu, C.L., 2004. A biological strategy for fabrication of Au/EGFP nanoparticle conjugates retaining bioactivity. Nano Lett. 4, 1209–1212.
Wang, Y., He, X., Wang, K., Zhang, X., Tan, W., 2009. *Barbated skullcup* herb extract-mediated biosynthesis of gold nanoparticles and its primary application in electrochemistry. Colloids Surf. B 73, 75–79.
Yoo, H.S., Lee, K.H., Oh, J.E., Park, T.G., 2000. In vitro and in vivo anti-tumor activities of nanoparticles based on doxorubicin–PLGA conjugates. J. Controlled Release 68, 419–431.
Zhang, Q., Yu, P., Li, Z., Zhang, H., Xu, Z., Li, P., 2003. Antioxidant activities of sulfated polysaccharide fractions from *Porphyra haitanesis*. J. Appl. Phycol. 15, 305–310.
Zhang, Z., Zhang, Q., Wang, J., Zhang, H., Niu, X., Li, P., 2009. Preparation of the different derivatives of the low-molecular-weight porphyran from Porphyra haitanensis and their antioxidant activities in vitro. Int. J. Biol. Macromol. 45, 22–26.